Journal of Pharmacokinetics and Biopharmaceutics, Vol. 19, No. 2, 1991

Physiologic and Metabolic Influences on Enterohepatic Recirculation: Simulations Based Upon the Disposition of Valproic Acid in the Rat

Gary M. Pollack[1,2] and Kim L. R. Brouwer[1]

Received October 4, 1990—Final October 4, 1990

The potential influence of alterations in several physiologic processes (hepatocellular egress, biliary excretion, gastrointestinal transit) and biotransformation steps (oxidative metabolism, glucuronidation) on the disposition of agents subject to significant enterohepatic recirculation (ER) via the glucuronide conjugate was examined in a series of simulation experiments. The model of ER developed was based upon the disposition of valproic acid (VPA) and valproate glucuronide (VPA-G) in the rat. The systemic disposition of VPA was simulated following changes in several processes contributing to (or competing with) ER: hepatic oxidative metabolism, hepatic glucuronidation, sinusoidal egress of glucuronide conjugate, canalicular egress of glucuronide conjugate, and gastrointestinal transit. Changes in the formation clearance of VPA-G resulted in a less than proportional change in systemic clearance of VPA, whereas changes in oxidative metabolism led to a greater than proportional change in systemic clearance. Furthermore, alterations in hepatocellular egress of VPA-G affected the disposition of the parent compound, suggesting that drug interactions or disease state effects on metabolite transport may be misinterpreted as effects at the level of metabolite formation. Analytical methods are proposed to recover the intrinsic kinetic parameters (formation clearances of metabolites, renal clearance of parent, volume of distribution) in the presence of ER from the systemic disposition of the parent alone.

KEY WORDS: enterohepatic recirculation; reabsorption; valproic acid; glucuronidation; biliary excretion.

INTRODUCTION

It has become increasingly apparent that enterohepatic recirculation (ER) is a significant dispositional process for many xenobiotics undergoing glucuronidation in the liver. ER has been documented for several agents of therapeutic and toxicologic interest in several mammalian species. Compounds that undergo significant recirculation via this route include morphine

[1]Division of Pharmaceutics, School of Pharmacy, The University of North Carolina at Chapel Hill, CB #7360, Chapel Hill, North Carolina 27599-7360.
[2]To whom correspondence should be addressed.

0900-466X/91/0400-0189$06.50/0

(1), diflunisal (2), benzodiazepines (3,4), valproic acid (VPA) (5) and its putative hepatotoxic metabolite (4-en-VPA) (6), methotrexate (7), indomethacin (8), the epoxide metabolite of benzo[*a*]pyrene (9), and the plasticizer tri-*p*-cresyl phosphate (10).

Recirculation of xenobiotic (most often mediated by the glucuronide conjugate) via the hepatobiliary/gastrointestinal system is an important pharmacokinetic phenomenon for several reasons. In the presence of such recirculation, pharmacokinetic processes that are normally associated with irreversible removal of xenobiotic from the systemic circulation (i.e., glucuronidation and biliary excretion) serve to transfer xenobiotic to a peripheral pharmacokinetic compartment (i.e., parent drug as the glucuronide conjugate in bile and gut lumen). Thus, changes in these processes induced by other drugs, environmental contaminants, or physiologic perturbations may not result in the anticipated changes in systemic disposition of the xenobiotic undergoing recirculation. Furthermore, the numerous sequential processes involved in ER (glucuronidation, biliary excretion of the glucuronide conjugate, gastrointestinal transport of the conjugate, hydrolysis of the conjugate, absorption of the liberated parent) result in a pharmacokinetic system with the potential for multiple drug and disease state interactions. ER prolongs the presence of drug within the systemic circulation, which may have therapeutic and/or toxicologic implications. Finally, ER repeatedly exposes selected organ systems, most notably the liver and gastrointestinal tract, to high concentrations of xenobiotic, potentially enhancing local toxicity (11).

The present investigation was undertaken to examine the systemic kinetics of a xenobiotic undergoing significant ER. Initial experiments were performed to examine the disposition of VPA and valproate glucuronide (VPA-G) in the rat in the presence and absence of ER. These experiments provided baseline kinetic parameters for the ER model. Parameters in the model were varied systematically in a series of simulation experiments to examine the effects of each parameter on systemic disposition of the parent compound and excretion of biotransformation products. In addition, based on data from these simulation experiments, analytical approaches were developed to determine intrinsic pharmacokinetic parameters (formation clearances of metabolites, renal clearance, apparent volume of distribution) in the presence of a recirculatory process.

THEORETICAL

The scheme depicting the ER model employed in the present study is presented in Fig. 1. This scheme was developed to describe the disposition of VPA in the rat, and therefore does not contain a gallbladder. The parent

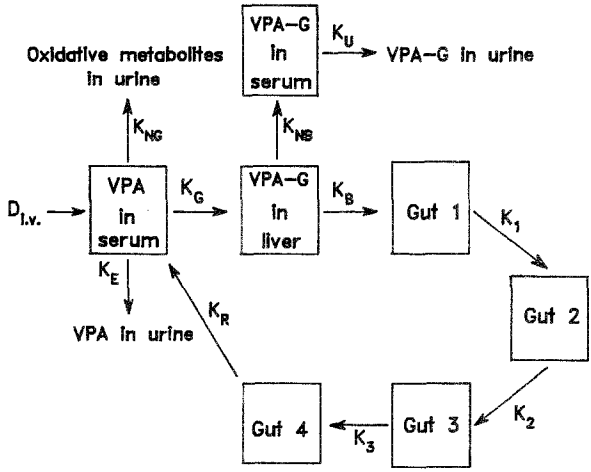

Fig. 1. Scheme depicting the model of ER developed to describe the disposition of VPA and VPA-G in the rat. This scheme represents the standard configuration of the ER model used in all simulations except those examining the influence of the number of hypothetical compartments in the ER loop (Gut 1–Gut 4). See text for explanation of symbols.

drug distributes within a single pharmacokinetic compartment with a volume V_c, yielding serum drug concentrations P_s. Drug is eliminated from the compartment via two metabolic routes, glucuronidation in the liver (with a rate constant K_G) and a nonglucuronidation metabolic process (with a rate constant K_{NG}). The elimination represented by K_{NG} may be either a single biotransformation process (with the exception of biliary excretion of unchanged parent drug) or the sum of several such processes. For the case of VPA, K_{NG} would represent oxidative metabolism in both the mitochondria and the microsomes (12,13). All elimination via the process(es) represented by K_{NG} is assumed to result in the eventual appearance of parent biotransformation products in the urine; the sum of these products is represented by $X_{u,ng}$. VPA may also be eliminated from the systemic circulation directly into the urine as unchanged drug, with a rate constant of K_E and cumulative amount appearing in the urine represented by $X_{u,p}$. The biliary excretion of unchanged VPA is insignificant (<10% of total biliary products) and has been ignored in the current model. Glucuronide conjugates of VPA formed within the liver (G_L) may be eliminated by one of two routes, either biliary excretion (with a rate constant K_B) or sinusoidal egress and ultimate renal excretion (with a rate constant K_{NB}). The renal excretion of VPA-G results in accumulation of the glucuronide conjugate in the urine ($X_{u,g}$).

VPA-G excreted in the bile is transported through the hepatobiliary/gastrointestinal tract to the eventual site of reabsorption. The present model incorporates four compartments to describe this portion of the recirculatory process. The optimal number of compartments was determined empirically to provide the best description of the concentration-time profile for VPA in the rat (see Generation of Parameter Estimates below). The influence of the number of gut compartments on the disposition profile was addressed in the present study, and the relevant simulations have been included (see Results). Physiologically, the four compartments may be viewed as representing conjugate in the bile within the liver (g1), conjugate in the bile duct (g2), conjugate at an initial nonhydrolytic site in the gastrointestinal tract (g3), and conjugate at the site of hydrolysis within the gastrointestinal tract (g4). In theory, the transport process associated with each hypothetical compartment in the recirculatory loop would have a unique rate constant. However, in practice it is not possible to resolve these rate constants from systemic concentration-time data. Therefore, the rate constants K_1 through K_3 were assumed to be equal in all simulations. At the end of the recirculatory process, parent drug can be reabsorbed into the central compartment (with a rate constant K_R) or can be lost to fecal elimination (with a rate constant K_{NR}). Both hydrolyzed parent drug and glucuronide conjugate may be excreted in the feces (producing a mass $X_{f,p+g}$ due to incomplete hydrolysis and/or incomplete absorption of liberated drug. Preliminary experiments with ^{14}C-labeled VPA indicated that essentially 100% of the administered dose appeared in the urine (unpublished data). K_{NR} was therefore set to zero in all simulations.

The model equations describing the ER system were written as Laplace transforms according to the approach described by Rescigno and Segre (14). For compartments containing no drug at time zero, the Laplace transform for drug content in each compartment was written as the transform of the rate of drug input into the compartment (i.e., the product of the rate constant entering the compartment and the Laplace transform of the drug content in the preceding compartment) divided by the sum of the rate constants exiting the compartment plus the Laplace operator s. Using this approach, the flux of drug through each compartment, with the exception of the central compartment, was described as follows:

Drug in the liver as glucuronide conjugate

$$L(G_L) = \frac{K_G \cdot L(P_s)}{s + K_B + K_{NB}} \tag{1}$$

where $L(G_L)$ is the Laplace transform for glucuronide conjugate in the

liver, $L(P_s)$ is the Laplace transform for parent drug in the central compartment, s is the Laplace operator, and all rate constants are as defined in Fig. 1. Similarly, the Laplace transforms for each gut compartment may be written as

Drug in the first gut compartment

$$L(\text{g1}) = \frac{K_B \cdot L(G_L)}{s + K_1} \tag{2}$$

Drug in the second gut compartment

$$L(\text{g2}) = \frac{K_1 \cdot L(\text{g1})}{s + K_2} \tag{3}$$

Drug in the third gut compartment

$$L(\text{g3}) = \frac{K_2 \cdot L(\text{g2})}{s + K_3} \tag{4}$$

Drug in the fourth gut compartment

$$L(\text{g4}) = \frac{K_3 \cdot L(\text{g3})}{s + K_R} \tag{5}$$

To describe adequately the disposition of unchanged parent drug in the central compartment, both input at time zero (the iv dose) and re-input from the ER process must be considered. The Laplace transform for parent in the central compartment resulting from the direct administration of the drug is

$$L(P_{s,d}) = \frac{D/V_c}{s + K_G + K_{NG} + K_E} \tag{6}$$

where $L(P_{s,d})$ is the Laplace transform of serum drug concentrations due to the administration of drug and D/V_c is the initial condition for the transform. Employing the approach described above, the Laplace transform for drug concentrations in the central compartment due to ER $[L(P_{s,R})]$ is

$$L(P_{s,R}) = \frac{K_R \cdot L(\text{g4})}{s + K_G + K_{NG} + K_E} \tag{7}$$

Since drug content in the central compartment is the only variable subject to experimental determination, it is necessary to solve Eq. (7) to calculate the Laplace transform directly from the characteristic rate constants for the system, the volume of the central compartment, and the administered dose.

The solution of this problem is obtained by substituting sequentially each of Eqs. (1) through (6) into the subsequent equation in the series to obtain an expression for $L(g4)$. This Laplace transform may then be substituted into Eq. (7). Upon simplification, this approach yields

$$L(P_{s,R}) = \frac{K_G \cdot K_B \cdot K_1 \cdot K_2 \cdot K_3 \cdot K_R \cdot L(P_s)}{\prod_{i=1}^{6} (s + E_i)} \tag{8}$$

where E_i is the sum of all rate constants exiting the ith compartment. Compartments through which VPA fluxes (as parent drug or glucuronide conjugate that has the *potential* to be converted back to parent drug) are numbered 1 through 6, beginning with the compartment representing parent in serum and ending with the fourth gut compartment. Since VPA-G in serum is assumed to be unable to reenter the liver, this compartment does not participate in ER of the parent and is therefore not included in this numbering scheme. Now, the Laplace transform for drug concentrations in the central compartment due to both administration and ER may be written as the sum of Eqs. (6) and (8). Isolating $L(P_s)$ and simplifying yields

$$L(P_s) = \frac{D/V_c \cdot [\prod_{i=1}^{6} (s + E_i)]}{(s + K_G + K_{NG} + K_E)[\prod_{i=1}^{6} (s + E_i) - \prod_{i=1}^{6} (H_i)]} \tag{9}$$

where H_i is the rate constant exiting the ith compartment that participates in the ER process.

In addition to the time course of drug in the central compartment, it is important to consider the elimination of drug by each route. This information is required for the classic calculation of partial clearances (renal clearance, formation clearance of metabolites). If hydrolysis within and absorption from the gastrointestinal tract are assumed to be complete, drug will be eliminated irreversibly from the system only by the kidneys, in either intact ($X_{u,p}$), glucuronidated ($X_{u,g}$), or nonglucuronidated ($X_{u,ng}$) forms. The Laplace transform for accumulation of nonglucuronidated drug in the urine is

$$L(X_{u,ng}) = \frac{K_{NG} \cdot L(P_s) \cdot V_c}{s} \tag{10}$$

Using the final value theorem of Laplace transforms, the eventual value of $X_{u,ng}$ at time infinity may be estimated from the product of s and $L(X_{u,ng})$ evaluated at $s = 0$. Therefore

$$X_{u,ng} = \frac{K_{NG} \cdot K_G \cdot K_B \cdot K_1 \cdot K_2 \cdot K_3 \cdot K_R \cdot D}{(K_G + K_{NG} + K_E)[\prod_{i=1}^{6} E_i - \prod_{i=1}^{6} H_i]} \tag{11}$$

A similar approach may be taken to determine the eventual amount of unchanged parent drug excreted in the urine ($X_{u,p}$). The amount of VPA-G

appearing in the urine may then be calculated as

$$X_{u,g} = D - X_{u,ng} - X_{u,p} \tag{12}$$

METHODS

Animal Experimentation

Silicone rubber cannulas were implanted in the right jugular veins of ether-anesthetized male Sprague-Dawley rats (300 to 350 g, $n = 5$) 24 hr prior to the experiment. VPA (di-*n*-propylacetic acid, Sigma Chemical Co., St. Louis, MO) dissolved in 2 N NaOH with *p*H adjustment to 7.5 with 3 N HCl, was injected as a 75 mg/kg bolus through the cannula. The 75 mg/kg dose is within the linear range of VPA disposition in the rat (5). Blood samples (0.3 ml) were withdrawn from the cannula at timed intervals for 30 hr. Animals were housed individually in polypropylene metabolic cages for the collection of urine samples (at timed intervals for 48 hr following drug administration).

To assess the disposition of VPA in the absence of ER, bile flow was exteriorized in a separate group of animals. Male Sprague-Dawley rats (285 to 325 g) were anesthetized with ethylcarbamate (1 g/kg), and body core temperature was maintained at 37°C with a heating pad, temperature controller, and rectal temperature probe. Polyethylene (PE-10) and silicone rubber cannulas were implanted in the bile duct and right jugular vein, respectively. Following a 30-min equilibration period, a bolus dose of VPA (75 mg/kg) was injected through the jugular vein cannula, and timed blood samples (0.3 ml) were withdrawn from the cannula for 3 hr.

Since VPA evidences concentration-dependent protein binding (15), a separate experiment was performed to assess the binding of VPA to proteins in rat serum. VPA was added *in vitro* to serum obtained from naive male rats in concentrations ranging from 10 μg/ml to 1000 μg/ml. Aliquots (1 ml) of serum were placed in Amicon (Danvers, MA) ultrafiltration devices equipped with YMT membranes, and were centrifuged at $700 \times g$ for 5 min. Temperature was maintained at 37°C throughout centrifugation. This centrifugation procedure provided approximately 80 μl ultrafiltrate. Unbound and total VPA concentrations were assessed in the ultrafiltrate and serum compartments, respectively. The binding parameters determined from this *in vitro* experiment were used to estimate the *in vivo* concentration of unbound VPA for the purposes of pharmacokinetic analysis. To determine the potential interanimal variability in binding of VPA to serum proteins, serum was collected from 6 naive male rats and VPA was added *in vitro* to produce concentrations of 50 μg/ml. The unbound fraction of VPA, determined as described above, was 0.326 ± 0.042. The relatively small coefficient

of variation (13%) suggests that the interanimal variability in binding of VPA to serum proteins is low, and that the binding constants derived from pooled serum data should describe VPA binding in individual animals reasonably well.

Analysis of VPA and VPA-G

Concentrations of VPA in serum, ultrafiltrate, and urine were determined using a modification of the gas-liquid chromatographic procedure of Loscher (16). Briefly, biological samples (25 to 100 μl) were acidified with an equal volume of 0.5 N HCl. VPA was extracted into 100 μl of chloroform containing cyclohexanecarboxylic acid (CCA) as an internal standard. Aliquots (1 to 3 μl) of the organic phase were injected onto a wide-bore fused silica capillary column (15 m × 0.53 mm i.d.) with FFAP as the bonded stationary phase (Alltech Associates, Deerfield, IL). The carrier gas (helium) was delivered at a rate of 10 ml/min, and the column temperature was maintained at 120°C. Analyte in the effluent carrier gas stream was detected by flame ionization. Under these conditions, the retention times of VPA and the internal standard were 4.2 and 6.0 min, respectively. Both compounds were resolved from the primary oxidative metabolites of VPA and endogenous components of serum and urine. The relationship between peak area ratios (VPA to CCA) and VPA concentration was linear at concentrations below 1000 μg/ml. The intraday coefficient of variation of the assay was less than 6% over the entire concentration range, and did not vary with sample concentration. The limit of detection was 0.1 μg/ml. Total (unchanged plus conjugated) VPA was determined following alkaline hydrolysis of VPA-G. Serum or urine samples were added to an equal volume of 2.5 N NaOH, incubated for 2 hr at 90°C, and acidified with 3 N HCl prior to extraction as described for the unchanged parent compound. The concentration of VPA-G in each sample was estimated from the difference between concentrations in hydrolyzed and unhydrolyzed samples.

Generation of Parameter Estimates

Several pharmacokinetic parameters in the ER model were obtained from the data collected in the initial animal experiment. The volume of distribution of unbound VPA was taken as the ratio of the administered dose to the initial serum concentration of unbound VPA. The actual activity of all clearance processes (CL_1) for unbound VPA (i.e., the total systemic clearance of the drug if recirculation was not present) was defined as the ratio of VPA dose to the area under the unbound concentration vs. time curve (AUC) prior to the recirculatory peak and extrapolated to time infinity

using the slope of the prerecirculatory concentration-time profile. The validity of this approach is demonstrated by the close correspondence between serum VPA concentrations in the prerecirculatory phase in intact animals and concentrations in rats with exteriorized bile flow (Fig. 2). The half-life of VPA in the prerecirculatory phase (or in bile duct-cannulated rats) was approximately 0.25 hr. In contrast, the half-life of VPA in the terminal disposition phase in intact animals, which was controlled primarily by the kinetics of recirculation, was 4.7 hr.

CL_1 represents the sum of metabolite formation clearances and renal clearance of the parent. Initial estimates of renal clearance of parent drug and formation clearance of the glucuronide conjugate were obtained in the usual manner (i.e., by multiplying CL_1 by the fraction of the administered dose excreted in the urine as unchanged parent or glucuronide conjugate). The combined formation clearance of all oxidative metabolites was estimated as the difference between CL_1 and the sum of renal and glucuronidation clearances. The validity of this traditional approach to estimate clearances in the presence of ER has yet to be established; examination of this issue was a primary objective of the present investigation. In any event, these estimates merely served as starting values for the parameters in the ER model. The clearance parameters estimated as described above were divided by V_c to obtain values for the rate constants used in model simulations (Table I). Absorption of VPA from the gastrointestinal tract is rapid (17), and the absorption rate constant (K_R) was taken to be 10 hr^{-1}. The rate constants for the canalicular (K_B) and sinusoidal (K_{NB}) egress of VPA-G were determined by changing the values of these constants in the model manually and examining the sum of squared errors of model predictions relative to the serum concentration and urinary excretion rate data for VPA and VPA-G. The rate constants for transit of VPA-G through the recirculatory loop (K_1 through K_3) were assumed to be equal, and were estimated by fitting the recirculatory model described above to the serum concentration-time data and the urinary excretion rate data for VPA and VPA-G. The optimal number of recirculatory compartments was determined by fitting models with different numbers of compartments to the collected data, and examining the Akaike's Information Criterion (18) for each model.

The fit of the recirculatory model to the serum and urine data for VPA and VPA-G, using parameter estimates determined as described above, is displayed in Fig. 2. The combination of parameter estimates listed in Table I (Simulation 1) used to generate the smooth curves yielded a reasonably good description of the experimental data. It should be noted that this set of parameters does not necessarily represent the true value (or even the best value) for each process. However, the model as a whole provides a reasonable description of the dispositional behavior of the compounds

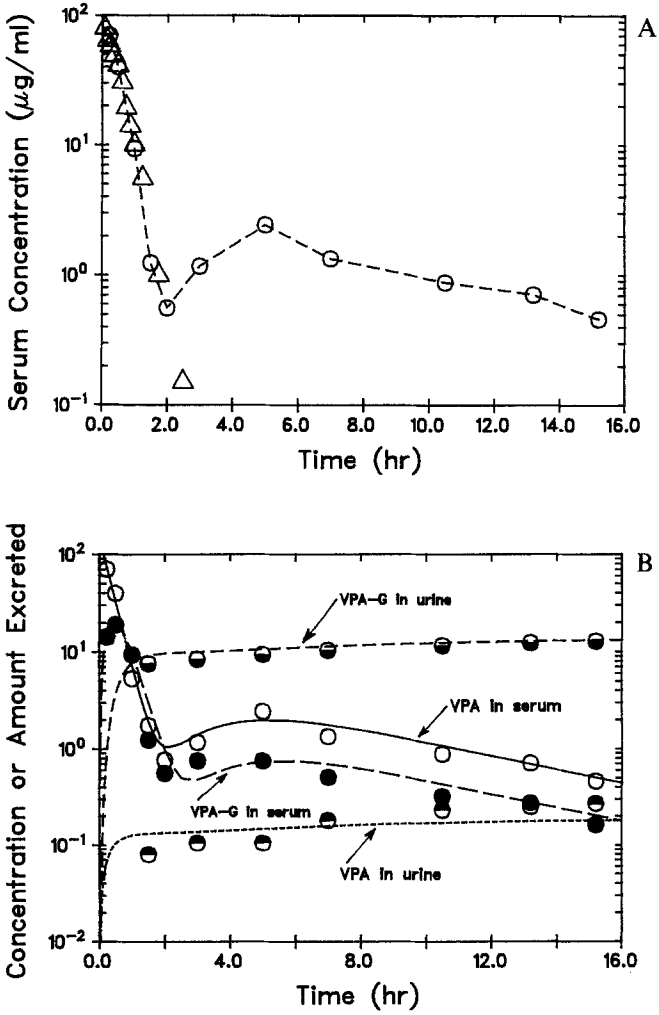

Fig. 2. A. Comparison of VPA serum concentration-time data in intact rats (circles) and rats with exteriorized bile flow (triangles); B. Fit of the ER model displayed in Fig. 1 to the concentration (μg/ml) vs. time and cumulative urinary excretion (mg) vs. time profiles for VPA and VPA-G. Data points represent the mean of 5 animals; error bars have been omitted for clarity. Lines indicate the best fit of the model to the data with the combination of parameters listed in Table I, Simulation 1.

Table I. Parameter Values Used in Enterohepatic Recirculation Simulation Experiments[a]

Simulation	K_G	K_{NG}	K_B	K_{NB}	K_1	K_2	K_3	K_R
1[b]	2.2	0.8	4.0	6.0	0.5	0.5	0.5	10
2	2.7	0.3	4.0	6.0	0.5	0.5	0.5	10
3	0.3	2.7	4.0	6.0	0.5	0.5	0.5	10
4	2.2	0.8	9.0	1.0	0.5	0.5	0.5	10
5	2.2	0.8	1.0	9.0	0.5	0.5	0.5	10
6	2.2	0.8	4.0	6.0	0.1	0.1	0.1	10
7	2.2	0.8	4.0	6.0	1.0	1.0	1.0	10
8	0.2	0.8	4.0	6.0	0.5	0.5	0.5	10
9	0.8	0.8	4.0	6.0	0.5	0.5	0.5	10
10	5.0	0.8	4.0	6.0	0.5	0.5	0.5	10
11	10.0	0.8	4.0	6.0	0.5	0.5	0.5	10
12	2.2	0.1	4.0	6.0	0.5	0.5	0.5	10
13	2.2	0.4	4.0	6.0	0.5	0.5	0.5	10
14	2.2	1.6	4.0	6.0	0.5	0.5	0.5	10
15	2.2	4.0	4.0	6.0	0.5	0.5	0.5	10
16	2.2	0.8	0.5	6.0	0.5	0.5	0.5	10
17	2.2	0.8	2.0	6.0	0.5	0.5	0.5	10
18	2.2	0.8	8.0	6.0	0.5	0.5	0.5	10
19	2.2	0.8	16.0	6.0	0.5	0.5	0.5	10
20	2.2	0.8	4.0	0.5	0.5	0.5	0.5	10
21	2.2	0.8	4.0	3.0	0.5	0.5	0.5	10
22	2.2	0.8	4.0	12.0	0.5	0.5	0.5	10
23	2.2	0.8	4.0	20.0	0.5	0.5	0.5	10
24[c]	2.2	0.8	4.0	6.0	—	—	—	0.164
25[d]	2.2	0.8	4.0	6.0	0.167	—	—	10
26[e]	2.2	0.8	4.0	6.0	0.333	0.333	—	10
27[f]	2.2	0.8	4.0	6.0	0.667	0.667	0.667	10
28[c]	2.2	0.8	4.0	6.0	—	—	—	0.0164
29[c]	2.2	0.8	4.0	6.0	—	—	—	1.64
30[f]	2.2	0.8	4.0	6.0	0.0667	0.0667	0.0667	10
31[f]	2.2	0.8	4.0	6.0	7.84	7.84	7.84	10
32	0.8	2.2	4.0	6.0	0.5	0.5	0.5	10
33	1.5	1.5	4.0	6.0	0.5	0.5	0.5	10
34	2.2	0.8	7.5	2.5	0.5	0.5	0.5	10
35	2.2	0.8	2.5	7.5	0.5	0.5	0.5	10
36	2.2	0.8	4.0	6.0	0.25	0.25	0.25	10
37	2.2	0.8	4.0	6.0	0.75	0.75	0.75	10

[a] Parameters are first-order rate constants with units of hr^{-1} as defined in the text; the values for the rate constants governing renal excretion of parent (K_E) and glucuronide conjugate (K_U) were held constant at 0.018 hr^{-1} and 3.5 hr^{-1}, respectively.

[b] Best set of parameter estimates to describe the actual disposition of valproate in the rat.

[c] Model contains one gastrointestinal compartment.

[d] Model contains two gastrointestinal compartments.

[e] Model contains three gastrointestinal compartments.

[f] Model contains five gastrointestinal compartments ($K_4 = K_1$).

under consideration, and therefore serves as a reasonable basis for examining the influence of each parameter on the disposition of the parent compound.

Influence of Kinetic Parameters on Disposition of the Parent Compound

The contribution of each parameter in the ER model to the overall disposition of VPA was assessed through a series of simulation experiments. Each parameter in the model was varied sequentially from the baseline value, and the resulting serum concentration-time profile was generated using the Laplace-solving computer program LAPLACE (MicroMath, Salt Lake City, UT). In addition, the urinary excretion of glucuronidated and nonglucuronidated products of VPA was assessed by solving Eqs. (11) and (12) directly. Thirty-seven simulations served as the basis for this investigation. The parameter values employed in each simulation are compiled in Table I. Simulations were conducted to examine the influence of the following aspects of the ER model on the disposition of parent drug: (i) routes of metabolism of VPA (Simulations 2, 3, 32, 33); (ii) routes of hepatic translocation of VPA-G (Simulations 4, 5, 34, 35); (iii) rate of transit through the recirculatory loop (Simulations 6, 7, 36, 37); (iv) inhibition or induction of hepatic glucuronidation (Simulations 8–11); (v) inhibition or induction of oxidative (nonglucuronidation) metabolism (Simulations 12–15); (vi) inhibition or induction of biliary excretion of VPA-G (Simulations 16–19); (vii) inhibition or induction of nonbiliary (sinusoidal) egress of VPA-G (Simulations 20–23); (viii) the number of apparent compartments in the recirculatory loop (Simulations 24–27); and (ix) rate of transit through the recirculatory loop for both the one (Simulations 24, 28, 29) and five (Simulations 27, 30, 31) recirculatory compartment models. Simulation 1 served as a control experiment for each of the cases cited above, with the exception of altering recirculatory loop transit in the one- and five-gut compartment models. In the experiments examining the contribution of different metabolic or excretory routes, the total elimination (i.e., $K_G + K_{NG}$ or $K_B + K_{NB}$) was held constant. These experiments, in addition to those involving alterations in the recirculatory loop, were directed towards assessing the types of dispositional differences that might be observed for various compounds that recirculate via biliary excretion of a glucuronide conjugate. In the inhibition/induction experiments, the total elimination for each product was allowed to change with the inhibition/induction of a particular pathway. These experiments were performed to examine the potential influence of disease states or drug interactions on recirculatory kinetics. The overall rate of transit through the recirculatory loop was held constant when the influence of number of recirculatory compartments on the disposition profile was examined.

Data Analysis

Simulated VPA concentration-time data were analyzed in traditional fashion (19) to obtain standard pharmacokinetic parameters. Total clearance (Cl_T) was calculated as the ratio of administered dose to AUC from time zero through infinity. Clearance in the absence of recirculation (Cl_1) was estimated from the AUC prior to the recirculatory peak, extrapolated to time infinity using the slope of the natural logarithm of concentration vs. time relationship in the prerecirculatory phase. The volume of the central compartment (V_c; i.e., the volume of the system in the absence of ER) was calculated as the ratio of dose to initial concentration. The steady-state volume of distribution ($V_{D^{ss}}$; i.e., the apparent volume of distribution in the presence of the recirculatory process) was estimated as

$$V_{D^{ss}} = \frac{D \cdot AUMC}{AUC^2} \tag{13}$$

where $AUMC$ (the first moment of the concentration-time curve) and AUC include the recirculatory peak and were extrapolated to time infinity. Mean residence times were estimated as the ratio of $AUMC$ to AUC. The percentage of the administered dose excreted in the urine as unchanged VPA, VPA-G, and oxidative metabolites ($X_{u,p}$, $X_{u,g}$, and $X_{u,ng}$, respectively) were used to calculate partial clearances (renal and metabolic). Several different approaches to estimating these partial clearances from urinary excretion data and the systemic disposition of the parent were evaluated (see Results). In each case, the estimated partial clearance was compared to the actual value used in the simulation (i.e., the product of the appropriate rate constant and V_c).

RESULTS

Experiment 1. Metabolism of Parent Compound

The influence of altering the relative magnitude of K_G and K_{NG}, while leaving their sum constant, on the simulated VPA concentration-time profile is displayed in Fig. 3. As the contribution of glucuronidation to total hepatic metabolism increased from 10% (Simulation 3) to 90% (Simulation 2), the total AUC increased due to increased ER. The disposition of VPA prior to the recirculatory peak was not dependent upon the fraction of the dose biotransformed to VPA-G. The pharmacokinetic parameters calculated for the five simulations in this experiment are compiled in Table II. Regardless of the relative magnitudes of the metabolic rate constants, analysis of the prerecirculatory concentration-time data provided the true (i.e., uncontaminated by the recirculatory process) apparent volume of distribution (V_c,

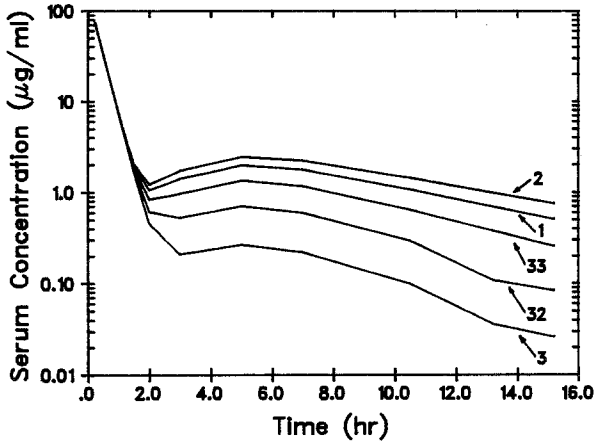

Fig. 3. Influence of altering the relative activities of metabolic routes on the disposition of VPA in serum. Data points were simulated at discrete time intervals and connected with straight lines; symbols representing data points have been omitted for clarity. Numbers indicate simulation number (refer to Table I for parameter values for each simulation).

actual value of 0.5 L/kg) and clearance (Cl_1, actual value of 1.5 L/hr/kg). The total systemic clearance in the presence of recirculation (Cl_T) decreased as the ratio of K_G to K_{NG} increased, due to increased ER. Similarly, the overall apparent volume of distribution ($V_{D^{ss}}$) increased with the extent of glucuronidation, indicating that the ER process serves as an apparent distributional space. Urinary excretion of metabolic products (glucuronide vs. oxidative metabolites) was not directly proportional to the activities of the two pathways. For example, when glucuronidation accounted for 10% of total metabolism, approximately 6% of the dose was recovered in urine as VPA-G. Thus, examination of urinary excretion would underestimate the true degree of conjugation by approximately 40% in this case. As the

Table II. Effects of Altering Metabolic Pathways on the Disposition of Valproic Acid

Simulation	K_G (hr^{-1})	K_{NG} (hr^{-1})	V_c (L/kg)	$V_{D^{ss}}$ (L/kg)	Cl_1 (L/hr/kg)	Cl_T (L/hr/kg)	$X_{u,g}$[a] (%)	$X_{u,ng}$[a] (%)	$X_{u,p}$[a] (%)
3	0.3	2.7	0.500	0.862	1.51	1.43	6.20	93.3	0.50
32	0.8	2.2	0.500	1.41	1.50	1.34	17.8	81.8	0.40
33	1.5	1.5	0.500	2.31	1.50	1.20	29.8	69.3	0.90
1	2.2	0.8	0.500	3.16	1.50	1.06	61.6	37.4	1.00
2	2.7	0.3	0.500	3.77	1.50	0.964	83.6	15.5	0.90

[a] Percentage of administered dose.

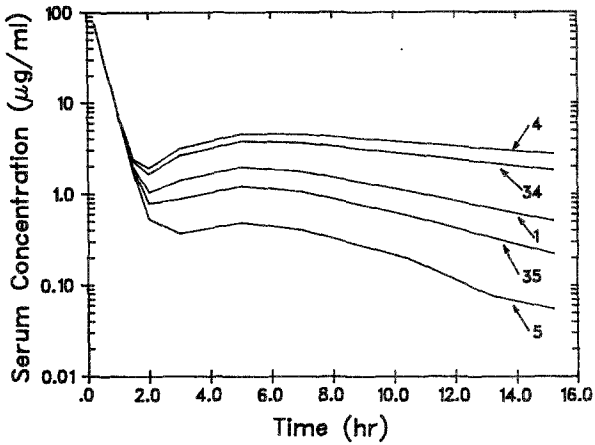

Fig. 4. Influence of altering the relative activities of hepatic excretory pathways for VPA-G on the disposition of VPA in serum. See Fig. 3 legend for details.

degree of glucuronidation increased (at the expense of oxidative metabolism) urinary content of VPA-G approached, but never achieved, the anticipated value.

Experiment 2. Hepatic Disposition of the Glucuronide Conjugate

The effect of altering the route by which VPA-G escapes the hepatocyte on the disposition of VPA is shown in Fig. 4. The total *AUC* increased as biliary excretion increased from 10% (Simulation 5) to 90% (Simulation 4) of the hepatic elimination of VPA-G. Changes in the biliary excretion of VPA-G altered the recirculatory peak, but did not affect the prerecirculatory disposition of VPA. The influence of changes in excretory pathways of VPA-G on the calculated pharmacokinetic parameters for VPA is displayed in Table III. As in the previous experiment, the true values for both V_c and

Table III. Effects of Altering Excretory Pathways for VPA-G on the Disposition of Valproic Acid

Simulation	K_B (hr^{-1})	K_{NB} (hr^{-1})	V_c (L/kg)	V_{D^∞} (L/kg)	Cl_I (L/hr/kg)	Cl_T (L/hr/kg)	$X_{u,g}{}^a$ (%)	$X_{u,ng}{}^a$ (%)	$X_{u,p}{}^a$ (%)
5	1.0	9.0	0.500	1.16	1.51	1.38	70.7	28.6	0.70
35	2.5	7.5	0.500	2.16	1.50	1.22	66.7	32.4	0.90
1	4.0	6.0	0.500	3.16	1.50	1.06	61.6	37.4	1.00
34	7.5	2.5	0.500	5.53	1.50	0.638	40.2	58.7	1.10
4	9.0	1.0	0.500	6.63	1.49	0.517	21.2	76.9	1.90

[a] Percentage of administered dose.

Cl_1 were obtained from the data prior to the secondary rise in concentration. Furthermore, Cl_T decreased, and $V_{D^{ss}}$ increased, as biliary excretion comprised an increasing fraction of hepatic disposition of VPA-G. It is noteworthy that although the relative contributions of the two metabolic pathways were held constant in this experiment, the pattern of metabolites excreted in the urine changed as hepatic disposition of VPA-G was altered. As biliary excretion of VPA-G increased, the percentage of the dose appearing in the urine as VPA-G decreased even though eventually 100% of the dose would be excreted in the urine in some form.

Experiment 3. Rate of Transit Through the ER Loop

The influence of transit time within the ER loop on the disposition of VPA is illustrated in Fig. 5. Increasing the rate constants comprising gut transit from 0.1 hr^{-1} (Simulation 6) to 1.0 hr^{-1} (Simulation 7) affected the shape of the disposition profile in several ways: the slope of the terminal phase increased, the maximum concentration in the ER peak increased, and the time to the ER peak decreased. However, both the prerecirculatory disposition and the total *AUC* were unchanged. The pharmacokinetic parameters derived from these simulations are compiled in Table IV. In general, gut transit had little influence on the kinetic parameters calculated for VPA, although $V_{D^{ss}}$ decreased markedly (from 14.4 to 1.83 L/kg) as transit rate increased.

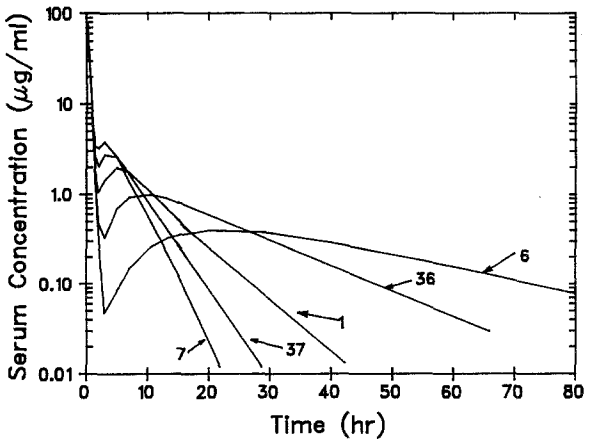

Fig. 5. Influence of altering the transit time through the recirculatory loop on the disposition of VPA in serum. See Fig. 3 legend for details.

Table IV. Effects of Altering Recirculatory Rate Constants on the Disposition of Valproic Acid[a]

Simulation	Rate constants (hr^{-1})	V_c (L/kg)	$V_{D^{ss}}$ (L/kg)	Cl_1 (L/hr/kg)	Cl_T (L/hr/kg)	$X_{u,g}$[b] (%)	$X_{u,ng}$[b] (%)	$X_{u,p}$[b] (%)
6	0.10	0.500	14.4	1.51	1.05	61.6	37.4	1.00
36	0.25	0.500	8.50	1.51	0.983	61.6	37.4	1.00
1	0.50	0.500	3.16	1.50	1.06	61.6	37.4	1.00
37	0.75	0.500	2.28	1.49	1.06	61.6	37.4	1.00
7	1.0	0.500	1.83	1.47	1.05	61.6	37.4	1.00

[a]The three rate constants in the ER loop (K_1, K_2, K_3) are assumed to be equal.
[b]Percentage of administered dose.

Experiment 4. Inhibition/Induction of Glucuronidation

The influence of changes in the formation clearance of VPA-G, as may occur secondary to physiologic perturbations or drug interactions, on the disposition of VPA is shown in Fig. 6. This experiment differs from Experiment 1 in that the formation clearance of oxidative metabolites was not adjusted to maintain a constant total metabolic clearance. As K_G increased from 0.2 hr^{-1} (Simulation 8) to 10.0 hr^{-1} (Simulation 11), the slope of the prerecirculatory disposition phase increased in the anticipated manner. The shape of the recirculatory peak also was affected by changes in formation clearance of VPA-G. At the two lowest levels of glucuronidation, no secondary rise in drug concentration was observed: the profiles were essentially biexponential. The kinetic parameters describing the disposition of VPA in this experiment are compiled in Table V. At each value of K_G, data in the

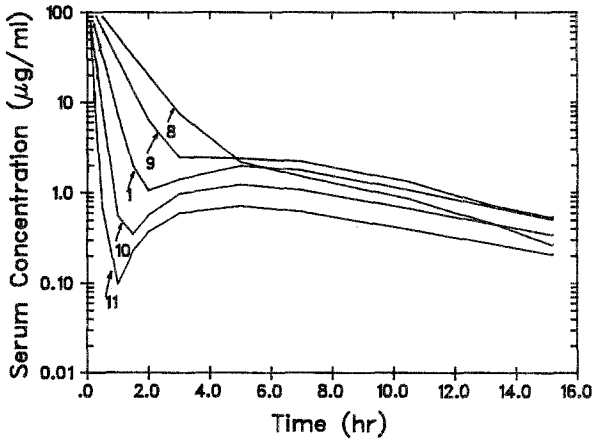

Fig. 6. Influence of inhibition or induction of glucuronidation on the disposition of VPA in serum. See Fig. 3 legend for details.

Table V. Effects of Inhibition/Induction of Glucuronidation on the Disposition of Valproic Acid

Simulation	K_G (hr^{-1})	K_{NG} (hr^{-1})	V_c (L/kg)	$V_{D^{ss}}$ (L/kg)	Cl_1 (L/hr/kg)	Cl_T (L/hr/kg)	$X_{u,g}$[a] (%)	$X_{u,ng}$[a] (%)	$X_{u,p}$[a] (%)
8	0.2	0.8	0.500	0.721	0.510	0.489	12.8	85.3	1.90
9	0.8	0.8	0.500	1.44	0.809	0.641	37.0	61.8	1.20
1	2.2	0.8	0.500	3.16	1.50	1.06	61.6	37.4	1.00
10	5.0	0.8	0.500	6.35	2.79	1.86	78.7	20.9	0.40
11	10.0	0.8	0.500	12.7	5.39	3.40	88.0	11.7	0.30

[a] Percentage of administered dose.

prerecirculatory phase provided an accurate estimate of V_C and Cl_1. However, Cl_T did not increase in parallel with Cl_1. The more than 10-fold increase in clearance incurred in changing K_G from 0.2 hr^{-1} to 1 hr^{-1} resulted in only a 7-fold increase in Cl_T. Furthermore, $V_{D^{ss}}$ increased as K_G increased. At low values of K_G, the urinary recovery of VPA-G underestimated the actual proportion of metabolic clearance directed towards glucuronidation by almost 40%. As K_G increased, the agreement between observed urinary output of VPA-G and the value predicted based upon known formation clearances improved (to an approximate 5% underprediction).

Experiment 5. Inhibition/Induction of Oxidative Metabolism

The effects of alterations in the formation clearance of oxidative metabolites on the disposition of VPA are displayed in Fig. 7. As in the previous

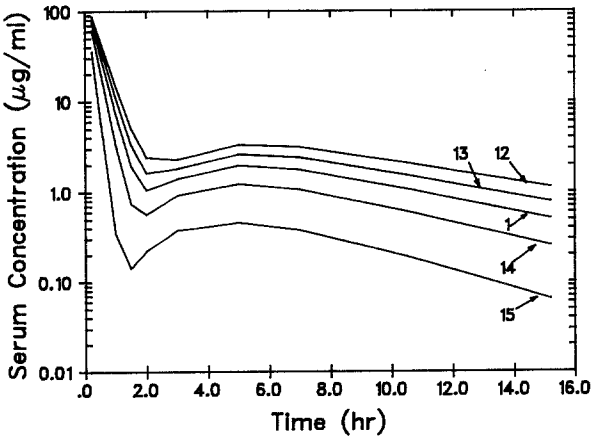

Fig. 7. Influence of inhibition or induction of oxidative metabolism on the disposition of VPA in serum. See Fig. 3 legend for details.

Table VI. Effects of Inhibition/Induction of Oxidative Metabolism on the Disposition of Valproic Acid

Simulation	K_G (hr^{-1})	K_{NG} (hr^{-1})	V_c (L/kg)	$V_{D^{ss}}$ (L/kg)	Cl_1 (L/hr/kg)	Cl_T (L/hr/kg)	$X_{u,g}$[a] (%)	$X_{u,ng}$[a] (%)	$X_{u,p}$[a] (%)
12	2.2	0.1	0.500	3.17	1.16	0.714	91.6	6.93	1.47
13	2.2	0.4	0.500	3.17	1.30	0.862	76.0	23.0	1.00
1	2.2	0.8	0.500	3.16	1.50	1.06	61.6	37.4	1.00
14	2.2	1.6	0.500	3.16	1.90	1.46	44.9	54.2	0.90
15	2.2	4.0	0.500	3.08	3.03	2.62	24.7	75.1	0.20

[a] Percentage of administered dose.

experiment, the activity of the alternate metabolic pathway was not adjusted to maintain a constant metabolic clearance. As K_{NG} increased from 0.1 hr^{-1} (Simulation 12) to 4.0 hr^{-1} (Simulation 15), the slope of the initial decline in serum concentrations increased and the total AUC decreased. The shape of the ER profile was similar in all cases. The pharmacokinetic parameters estimated in this experiment are presented in Table VI. Prerecirculatory data were sufficient to calculate V_c and Cl_1. Unlike previous experiments, however, $V_{D^{ss}}$ remained constant and was apparently insensitive to changes in the formation clearance of metabolites that do not contribute to ER of the parent. Cl_T increased more than would be predicted based upon the degree of change in formation clearance: Cl_1 increased 2.7-fold as K_{NG} increased from 0.1 hr^{-1} to 4.0 hr^{-1}, but Cl_T increased 3.7-fold. Urinary excretion of VPA-G underpredicted the contribution of glucuronidation to metabolic clearance, while the urinary excretion of oxidative metabolites overpredicted the contribution of oxidation. These overpredictions ranged from more than 50% at the lowest value of K_{NG} to approximately 16% at the highest value of K_{NG}.

Experiment 6. Inhibition/Induction of Biliary Excretion of VPA-G

The effect of perturbing biliary excretion of VPA-G on the systemic disposition of VPA is presented in Fig. 8. This experiment differed from Experiment 2 in that the sum of K_B and K_{NB} was not held constant. As K_B increased from 0.5 hr^{-1} (Simulation 16) to 16 hr^{-1} (Simulation 19) the area under the ER peak increased and the slope of the terminal phase decreased. The disposition of the drug prior to the ER peak was not affected. The pharmacokinetic parameters derived from these data are compiled in Table VII. Increasing K_B, as might occur due to induction of carrier proteins by xenobiotics, resulted in an increase in $V_{D^{ss}}$ and a decrease in Cl_T. Alterations in K_B also affected the pattern of metabolites appearing in the urine: as K_B increased, the urinary recovery of VPA-G decreased in favor

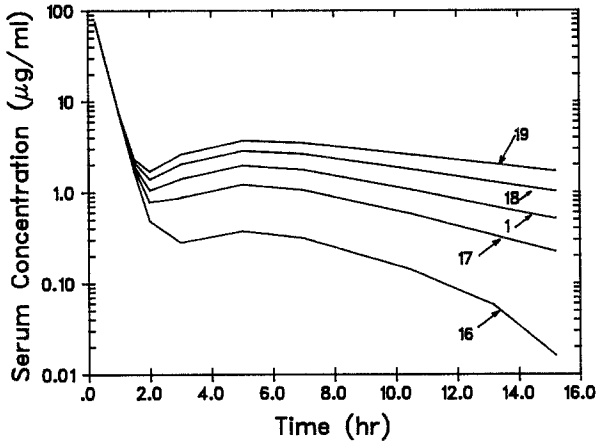

Fig. 8. Influence of inhibition or induction of VPA-G biliary excretion on the disposition of VPA in serum. See Fig. 3 legend for details.

of oxidative metabolites. Thus, events that impinge upon the biliary disposition of the conjugate would appear, based upon systemic and urinary data alone, to affect metabolic routes.

Experiment 7. Inhibition/Induction of Sinusoidal Egress of VPA-G

The influence of alterations in the sinusoidal egress of VPA-G on the systemic disposition of VPA is displayed in Fig. 9. As K_{NB} increased from 0.5 hr^{-1} (Simulation 20) to 20 hr^{-1} (Simulation 23), the slope of the terminal phase increased and the *AUC* associated with the ER peak decreased. As was the case for K_B, the time at which the secondary rise in drug concentrations occurred was not affected markedly by K_{NB}. The pharmacokinetic parameters calculated from these simulated data are presented in Table VIII. In contrast to K_B, as K_{NB} increased $V_{D^{ss}}$ decreased and Cl_T increased.

Table VII. Effects of Inhibition/Induction of Biliary Excretion of VPA-G on the Disposition of Valproic Acid

Simulation	K_B (hr^{-1})	K_{NB} (hr^{-1})	V_c (L/kg)	$V_{D^{ss}}$ (L/kg)	Cl_1 (L/hr/kg)	Cl_T (L/hr/kg)	$X_{u,g}$[a] (%)	$X_{u,ng}$[a] (%)	$X_{u,p}$[a] (%)
16	0.5	6.0	0.500	0.926	1.51	1.42	71.1	28.1	0.80
17	2.0	6.0	0.500	2.17	1.50	1.22	66.7	32.4	0.90
1	4.0	6.0	0.500	3.16	1.50	1.06	61.6	37.4	1.00
18	8.0	6.0	0.500	4.33	1.50	0.874	53.3	45.3	1.40
19	16.0	6.0	0.500	5.35	1.50	0.707	42.3	56.4	1.30

[a] Percentage of administered dose.

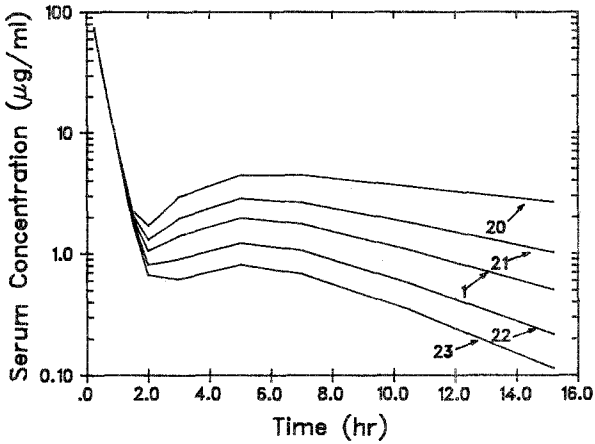

Fig. 9. Influence of inhibition or induction of sinusoidal excretion of VPA-G on the disposition of VPA in serum. See Fig. 3 legend for details.

Perturbation of this route of conjugate excretion also affected the pattern of metabolites excreted in urine; based on urinary data, changes in sinusoidal egress of VPA-G appeared to alter the metabolism of VPA.

Experiment 8. Alteration of the Number of Apparent Compartments in the Recirculatory Loop

The effect of the structure of the ER model on the shape of the concentration-time profile for VPA was investigated by altering the number of gut compartments from one to five. The rate constants for gut transport (and, for the case of a single compartment loop, the rate constant for absorption from the gut) were varied between models to maintain a constant residence time within the ER loop (Simulations 24–27). The results of this experiment are shown in Fig. 10. The particular structure of the model had

Table VIII. Effects of Inhibition/Induction of Sinsuoidal Excretion of VPA-G on the Disposition of Valproic Acid

Simulation	K_B (hr^{-1})	K_{NB} (hr^{-1})	V_c (L/kg)	$V_{D^{ss}}$ (L/kg)	Cl_I (L/hr/kg)	Cl_T (L/hr/kg)	$X_{u,g}$[a] (%)	$X_{u,ng}$[a] (%)	$X_{u,p}$[a] (%)
20	4.0	0.5	0.500	6.62	1.50	0.532	23.0	75.1	1.90
21	4.0	3.0	0.500	4.32	1.50	0.878	53.3	45.3	1.40
1	4.0	6.0	0.500	3.16	1.50	1.06	61.6	37.4	1.00
22	4.0	12.0	0.500	2.15	1.50	1.22	66.7	32.4	0.90
23	4.0	20.0	0.500	1.59	1.50	1.31	68.6	30.5	0.90

[a] Percentage of administered dose.

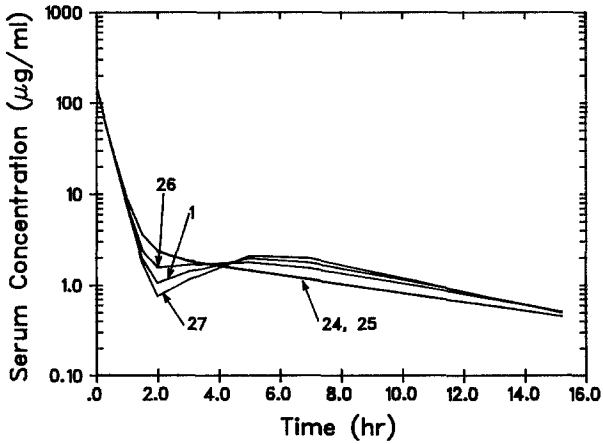

Fig. 10. Influence of changing the number of ER compartments on the disposition of VPA in serum. The biexponential profiles (Simulations 24 and 25) represent the one- and two-compartment loop systems.

little influence on the overall disposition of the parent drug, as is evidenced by the similarity of the profiles. However, in the case of both the one- and two-compartment recirculatory loops, the disposition profiles appeared to be biexponential and were identical. The pharmacokinetic parameters calculated from each of these simulations were identical to the standard case (Simulation 1).

The number of hypothetical compartments in the ER loop appeared to influence the presence or absence of a secondary rise in drug concentrations. To determine whether the shape of the disposition profile could be modulated further by the residence time within the ER loop, an additional set of simulations was performed to examine VPA disposition with varying residence times in both the one- and five-compartment ER loop models. These simulations are displayed in Fig. 11. In the case of the one-compartment ER system (Simulations 24, 28, 29) disposition profiles were biexponential regardless of the mean residence time for ER. However, the simulation performed with the shortest residence time (highest rate constant) had a very shallow initial phase. The apparent "distributive" phase became more marked, and the terminal phase less steep, as the residence time within the loop increased. In the case of the five-compartment ER system (Simulations 27, 30, 31), a rapid transit through the loop resulted in a biexponential decline similar to that observed for the one-compartment model. This particular profile appears to be monoexponential in Fig. 11 because of the narrow time scale for this simulation. As the residence time increased, the

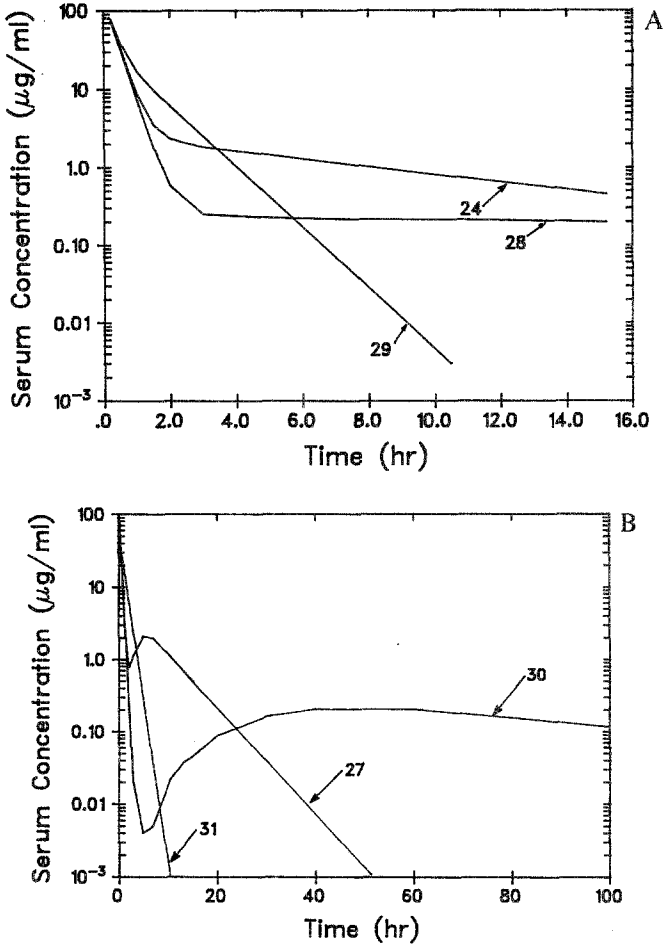

Fig. 11. Influence of altering ER transit time in the one-compartment (A) and five-compartment (B) loop systems. See Fig. 3 legend for details.

secondary rise in drug concentrations appeared and became more pronounced, and the slope of the terminal disposition phase decreased.

Calculation of Intrinsic Pharmacokinetic Parameters

It is clear from examination of the parameters listed in Tables II–VIII that standard pharmacokinetic approaches to data analysis in the presence of significant ER may provide inaccurate, and perhaps misleading, information. Several analytical approaches were evaluated to recover the intrinsic

pharmacokinetic parameters of the system, as well as to define the significance of the ER process itself.

Partial Clearances

Since oxidative metabolites of VPA are assumed not to contribute to ER, the production of oxidative metabolites should be dependent upon the formation clearance of these products (Cl_{OX}) and the systemic exposure to the precursor (AUC_T for VPA). Thus, if $X_{u,ng}$ represents total urinary excretion of oxidative metabolites, then Cl_{OX} may be calculated in the standard manner as

$$Cl_{OX} = \frac{X_{u,ng}}{AUC_T} \tag{14}$$

The relationship between the actual (i.e., in the absence of recirculation) formation clearance of oxidative metabolites ($K_{NG} \cdot V_c$) and the calculated values of Cl_{OX} [according to Eq. (14)] is presented in Fig. 12. The close correspondence between these values confirms that the traditional approach to estimating formation clearance is valid for metabolites that do not contribute to ER of the parent. Similar reasoning may be used to support calculation of renal clearance (Cl_R) of the parent as the ratio of mass of unchanged parent drug in urine to the total AUC.

In contrast to oxidative metabolites, it is not possible to calculate the formation clearance of the glucuronide conjugate (Cl_G) in the traditional

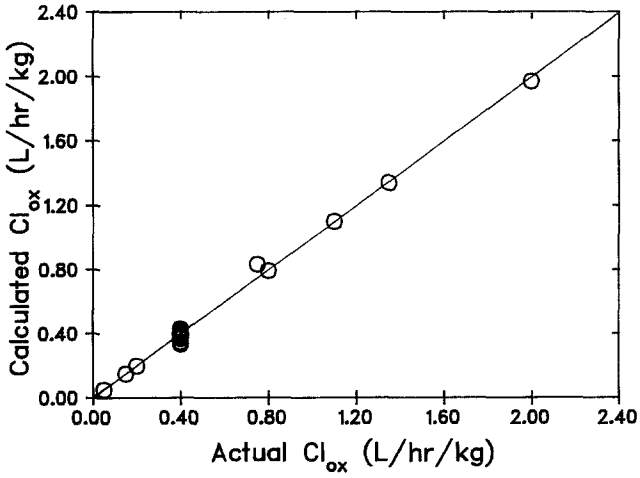

Fig. 12. Relationship between calculated (i.e., in the presence of ER) and actual (i.e., in the absence of ER) values for formation clearance of oxidative metabolites. Solid line represents the line of identitity.

manner ($X_{u,g}/AUC_T$) when the glucuronide is the species driving ER: in all cases, the actual value ($K_G \cdot V_c$) was underestimated. This result was expected since a certain fraction of the glucuronide conjugate formed is recirculated, and has the opportunity to reach the urine in the form of oxidative metabolites or parent. The only approach to estimating the formation clearance of the recirculating metabolite reliably is to subtract all other partial clearances (in this case, Cl_R and Cl_{OX}) from the true systemic clearance (Cl_1) (Fig. 13).

Fraction of Parent Undergoing Recirculation

The cumulative fraction of the administered dose undergoing recirculation (F_R) may be estimated from the total AUC (AUC_T) and the AUC in the absence of recirculation (AUC_1, the AUC prior to the recirculatory peak extrapolated to time infinity)

$$F_R = \frac{AUC_T - AUC_1}{AUC_1} \tag{15}$$

F_R may be related to the fraction undergoing a given recirculation (f_r, which in the present system is reflective of the relative magnitudes of K_G vs. K_{NG} and K_B vs. K_{NB}) as

$$F_R = f_r + f_r^2 + f_r^3 + \cdots \tag{16}$$

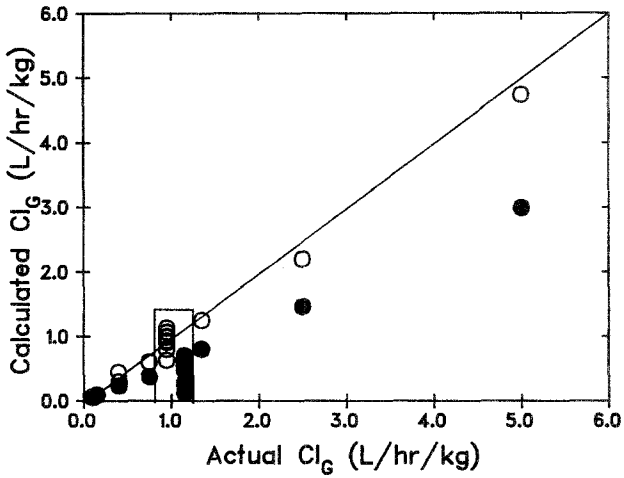

Fig. 13. Relationship between calculated and actual values for formation clearance of VPA-G (open circles = $Cl_1 - Cl_{OX} - Cl_R$; closed circles = X_G/AUC_T; see text for explanation of symbols). Solid line represents the line of identity. The box identifies simulations conducted at an actual Cl_G of 1.1 L/hr/kg; data points representing the two calculations of Cl_G have been offset for clarity.

The above summation reduces to

$$f_r + f_r^2 + f_f^3 + \cdots = \frac{f_r}{1 - f_r} \tag{17}$$

Equations (16) and (17) may be combined and rearranged to yield an expression allowing calculation of f_r from systemic concentration-time data for the parent compound

$$f_r = \frac{F_R}{1 + F_R} \tag{18}$$

The actual fraction of parent undergoing a given recirculation is the product of the fraction of parent that is glucuronidated and the fraction of the glucuronide conjugate that undergoes biliary excretion

$$f_r = \frac{K_G}{K_G + K_{NG} + K_E} \cdot \frac{K_B}{K_B + K_{NB}} \tag{19}$$

A comparison of calculated f_r vs. the actual value [based on Eq. (19)] is presented in Fig. 14. The good correspondence between these values suggests that estimation of f_r from AUC data for the parent is reliable, assuming that the onset of the ER process may be identified from systemic concentration-time data. It should be noted that if f_r and the fractional metabolic clearances are known, as calculated above, then the relative contributions

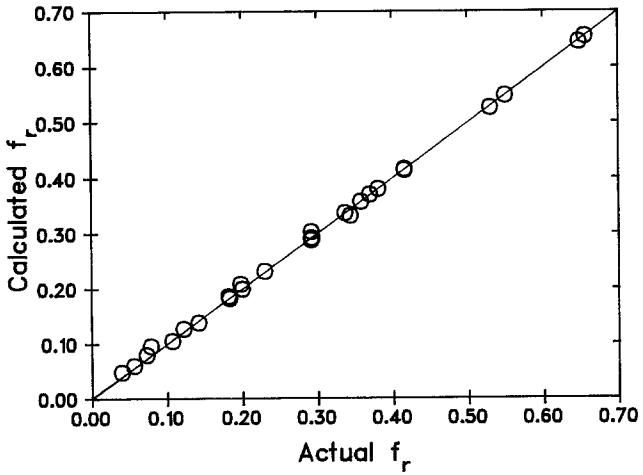

Fig. 14. Relationship between calculated and actual values for the fraction of VPA undergoing ER during any given pass. Solid line represents the line of identity.

of sinusoidal and canalicular egress of the glucuronide conjugate may be estimated. Thus, some information regarding the biliary excretion of a conjugate may be gained without obtaining bile samples or examining the disposition of the conjugate itself.

Apparent Volume of the ER Process

ER (particularly for VPA in the rat, where ER is 100% efficient) behaves as an additional distributive compartment. If, in the absence of ER, the body behaves as a single compartment, then the apparent volume of recirculation (V_R) may be calculated as

$$V_R = V_{D^{ss}} - V_c \tag{20}$$

where V_c is the ratio of dose to initial concentration and $V_{D^{ss}}$ is calculated according to Eq. (13). Similarly, the mean residence time within the recirculatory process (MRT_R) may be calculated as

$$MRT_R = MRT_T - MRT_I \tag{21}$$

where MRT_T is the ratio of $AUMC$ to AUC for the entire profile and MRT_I is the ratio of $AUMC$ to AUC for the pre-ER phase with extrapolation to time infinity. The validity of this calculation of recirculatory residence time is demonstrated in Fig. 15, where the actual recirculatory residence

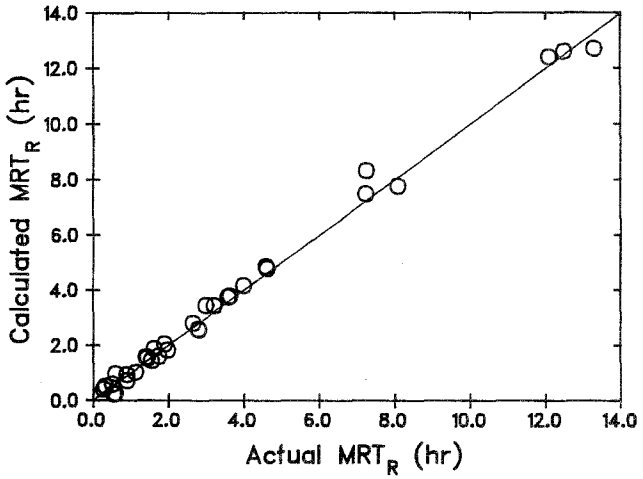

Fig. 15. Relationship between calculated mean residence time for recirculation [according to Eq. (21)] and the actual value for each simulation [according to Eq. (22)]. Solid line represents the line of identity.

time is

$$MRT_R = F_R \cdot T_R \tag{22}$$

F_R is calculated from Eqs. (16) and (19), and T_R, the transit time through the recirculatory loop, is calculated as the sum of the reciprocal of all the

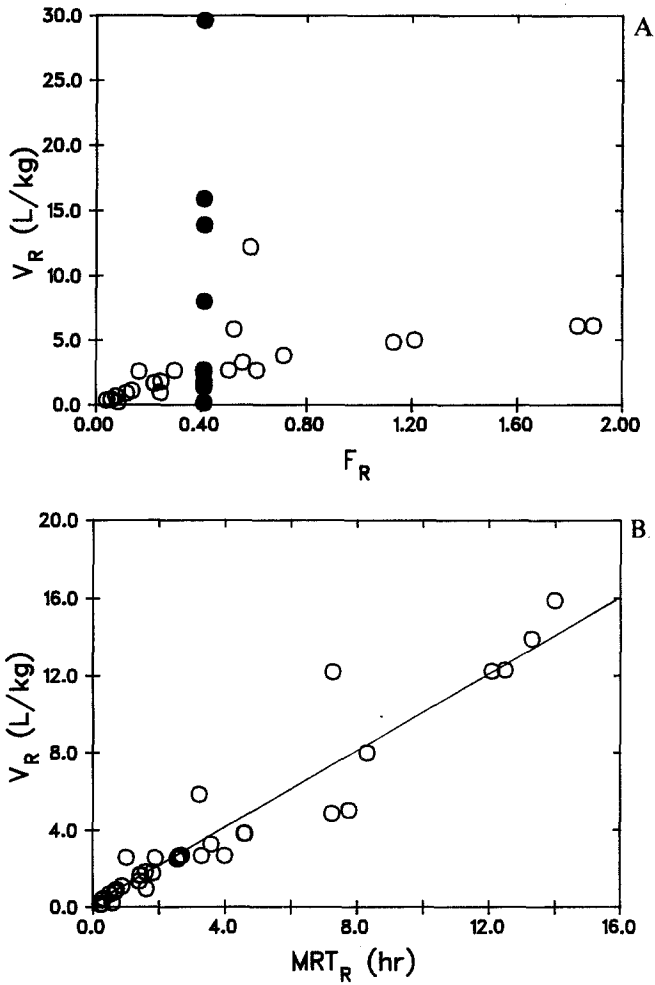

Fig. 16. Relationship between apparent volume of the recirculatory process and either the actual cumulative fraction of the dose recirculated (A) or the actual mean residence time within the ER loop (B). Solid circles in Panel A identify simulations in which loop residence time was varied. Solid line in Panel B indicates the results of linear regression of the data ($Y = 0.907 * X + 0.259$, $r^2 = 0.851$).

rate constants participating in ER (i.e., K_G, K_B, K_1, K_2, K_3, K_R). It was anticipated that V_R would be determined primarily by F_R (i.e., the total body load present in the ER loop). However, the relationship between V_R and F_R was not predictable across the entire set of simulations. Figure 16 demonstrates the rather weak correlation between V_R and F_R in comparison to the relationship between V_R and MRT_R. In all cases, including a variable recirculatory loop transit time, the apparent volume of the recirculatory process was related to recirculatory residence time.

DISCUSSION

The objective of the present study was the construction of a pharmacokinetic model to describe VPA disposition in the rat and to examine the influence of changes in various dispositional processes on the behavior of the model. The ER model, which is similar to a previously published scheme for morphine disposition in the rat (1), included systemic compartments for VPA and VPA-G, a hepatic compartment for VPA-G, and a four-compartment ER loop. The scheme depicted in Fig. 1 represents the simplest model that adequately described the disposition of both VPA and VPA-G in the rat.

The results of the present simulation experiments elucidated several fundamental aspects of the behavior of ER systems. When the glucuronide conjugate participates in ER, changes in the relative activities of glucuronidation and nonglucuronidation pathways do not result in equivalent changes in systemic clearance. In the present study, an increase in the formation clearance of VPA-G was partially offset by an increase in the fraction recycled, leading to a smaller than predicted increase in total systemic clearance (Table V). Conversely, an increase in the formation clearance of metabolites that do not participate in ER resulted in a larger than predicted increase in total clearance (Table VI). Induction of the oxidative metabolic pathway simultaneously increased systemic clearance and diverted drug from the ER process.

In each of the simulations performed, the pattern of urinary metabolite excretion was not equivalent to the relative activities of the metabolic pathways involved (Tables II, V, and VI). Thus, in the presence of ER involving the participation of a metabolite, urinary metabolite profiles may not reflect relative formation clearances. For example, in the inhibition/induction experiment for oxidative metabolism (Table VI), the fraction of the dose excreted in the urine as nonglucuronide metabolites overpredicted the relative activity of this route by as much as 55%. In contrast, the same experiment indicated that the fraction of the dose recovered as urinary

glucuronide conjugate underpredicted the relative activity of this metabolic route by as much as 44%.

In addition to its influence on systemic and apparent partial clearances, the formation clearance of the glucuronide conjugate affected the $V_{D^{ss}}$ of VPA. In most pharmacokinetic systems, distribution volume is assumed to be unrelated to clearance. The ER system is unusual in that a process normally resulting in irreversible removal of substrate from the system (i.e., glucuronidation) results in only partial removal of substrate. A fraction of the conjugate formed returns to the systemic circulation as parent. Thus, a clearance process has become, to a certain extent, a distributional process, and affects the apparent distribution volume accordingly. A similar observation has been made for the ergot alkaloid methylergometrine (20). Disruption of the ER process resulted in a significant decrease in the $V_{D^{ss}}$ of this compound.

Unlike standard linear pharmacokinetic systems, the disposition of a metabolite (in this case, VPA-G) in an ER system can influence the kinetics of the parent. Changes in the relative contributions of sinusoidal and canalicular excretion of VPA-G affected the disposition of VPA. In general, as biliary excretion of VPA-G increased relative to the nonbiliary route, the systemic clearance of VPA declined (Tables III, VII, VIII). Similarly, the apparent volume of the system was related to biliary excretion of the conjugate. As K_B increased (with respect to the sum of K_B and K_{NB}), $V_{D^{ss}}$ increased.

The influence of hepatobiliary disposition of the glucuronide conjugate on the recovery of metabolites in the urine is worthy of particular note. Since ER in the present model was assumed to be 100% efficient, changes in the relative contribution of biliary and nonbiliary excretion of VPA-G had no influence on the *total* fraction of the dose appearing in the urine as all metabolic products; eventually, the entire dose was recovered. In most kinetic systems, changes in the pattern of metabolites appearing in the urine reflect changes in metabolite formation clearance. It is clear from the present study that changes in the excretory processes for the glucuronide conjugate can influence urinary metabolite recovery. Increases in K_B resulted in decreased systemic clearance, decreased urinary recovery of glucuronide conjugate, and increased recovery of nonglucuronidated products (Table VII). Taken together, these observations lead to (i) the incorrect conclusion that the formation clearance of the glucuronide conjugate was inhibited and (ii) the correct conclusion that oxidative metabolism was unaffected. Thus, calculation of formation clearances in the usual manner may lead to erroneous inferences concerning the mechanism of drug or disease state interactions within an ER system. Interactions at the level of hepatic disposition of the conjugate may be interpreted as perturbations in

the formation of the conjugate. Furthermore, events that actually *induce* a clearance process (i.e., biliary metabolite clearance) may appear to *inhibit* metabolite formation.

The importance of this latter point may be demonstrated by considering the dose-dependent disposition of VPA in both rat and man. Previous experiments in this laboratory have indicated that the fraction of the dose of VPA appearing in the urine as VPA-G increased with increasing dose, although the apparent formation clearance of VPA-G decreased over the same dose range (21). A similar observation of dose-dependent urinary recovery of VPA-G, with no apparent change in total clearance of VPA, was reported recently in normal volunteers (22). These observations are difficult to interpret from a classic pharmacokinetic frame of reference. To explain the data obtained in rats, both oxidation and glucuronidation pathways must be saturable, with oxidation being more saturable than glucuronidation. In man, explanation of these observations is even more complex. Oxidative metabolism must evidence a dose-dependent decrease, while the formation clearance of glucuronide conjugates would have to *increase* with administered dose. A more plausible explanation involves saturable biliary excretion of the glucuronide conjugate in both species. The present series of simulations predicts that a decrease in K_B would produce an increased urinary recovery of VPA-G. Experiments are currently underway in this laboratory to confirm *in vivo* the model predictions of dose-dependency in the disposition of VPA.

With the exception of $V_{D^{ss}}$, changes in the structure of the ER process or the residence time within the ER loop had little influence on calculated pharmacokinetic parameters. However, changes in ER kinetics did affect the concentration-time profile of parent in the systemic circulation. Changing the recirculatory residence time, but leaving the number of compartments constant, did not eliminate the secondary rise in concentrations characteristic of ER (Fig. 5). However, decreasing the number of compartments in the ER loop to one or two eliminated the secondary peak entirely (Fig. 10). Thus, under certain conditions, a compound undergoing significant ER may appear to exhibit two-compartment behavior. For the one-compartment ER process, a secondary rise in concentrations could not be generated regardless of the recirculatory transit time (Fig. 11A). Even in the five-compartment system, a biexponential decline could be generated with a very brief ER residence time (Fig. 11B). Thus, ER may be a significant dispositional process even though a secondary peak in the systemic concentration-time profile for the parent is absent. Indeed, there are several examples in the literature of compounds that demonstrate significant recirculation in the absence of a secondary rise in concentrations, including diflunisal (2), lorazepam (3), temazepam (4), and doxycycline (23).

No combination of parameter values or ER loop structures yielded more than a single recirculatory peak. One explanation for the lack of multiple peaks is that the present model did not include a gallbladder (consistent with the anatomy of the rat). In an attempt to demonstrate multiple peaks for the VPA system, a gallbladder was added to the model and several simulations were performed (data not shown). Simulated concentration–time profiles evidenced no more than two secondary peaks. This behavior is in agreement with previous studies (24,25) but in contrast to some simulations predicting numerous symmetrical sequential peaks (26,27). It seems likely that the residence time in the gallbladder must be long with respect to all other kinetic processes in the system for multiple peaks to occur. This would allow the majority of the total body load of substrate (albeit in the form of the glucuronide conjugate) to collect within the gallbladder immediately prior to reentry into the systemic circulation. Although this may be true for some compounds, the majority of drug substances subjected to ER are associated with half-lives that are relatively long in comparison to gallbaldder emptying time.

It is clear from the foregoing discussion that standard techniques for resolution of intrinsic pharmacokinetic parameters are not applicable when significant ER occurs via a glucuronide conjugate. However, several alternate approaches may be taken to analyze data obtained from an ER system. The techniques employed in the present investigation are similar in some respects to those previously suggested for use in the presence of reversible metabolic processes (28–31). Proper analysis of ER data is limited by the ability to identify the time at which recirculated drug begins to appear in the systemic circulation. Such identification poses no particular problem when a recirculatory peak is evident in the concentration–time profile. However, in the case of ER with no clear secondary peak, additional information (e.g., disposition in the presence of diverted bile flow) is required to determine the time at which recirculated drug contributes significantly to systemic concentrations. In either case, if identification of the prerecirculatory phase can be made, the approaches outlined in the present communication allow recovery of several intrinsic pharmacokinetic parameters. Assuming the data in the pre-ER phase are sufficient, the true systemic clearance and apparent volume of distribution (uncontaminated by recirculation) may be estimated from these data alone; in essence, the pre-ER concentration–time data behave as if the organism has exteriorized bile flow. As demonstrated in Fig. 13, formation clearance of the glucuronide conjugate may only be estimated by subtracting all other partial clearances (formation clearances of nonrecirculating metabolites, renal clearance of the parent) from the true total clearance (i.e., defined by the pre-ER phase). All other methods of estimating glucuronide formation clearance

(glucuronide recovered in urine divided by either the pre-ER *AUC* or the total *AUC*) failed to recover the true value of this parameter in a significant number of simulations. In contrast, the formation clearance of metabolites not contributing to ER of the parent, as well as the renal clearance of the parent itself, may be estimated in the usual fashion (total urinary recovery divided by total *AUC*).

Analysis of systemic concentration-time data for the parent compound alone also can provide information regarding the extent of ER and, to some degree, the hepatobiliary disposition of the glucuronide conjugate. The *AUC* analysis presented in Eq. (15) allows estimation of the total mass of drug (relative to the administered dose) traversing the ER loop. The fraction of the parent compound undergoing ER at any given time (f_r) may then be calculated from Eq. (18). The good correspondence between calculated and actual values of f_r across all the simulations performed (Fig. 14) suggests that *AUC* analysis provides a reasonable estimate of ER fraction. If the partial clearances of the parent are determined as described above, the relative contribution of sinusoidal and canalicular excretion of the glucuronide conjugate may be determined according to Eq. (19). Although this would be a gross estimate of the hepatobiliary disposition of the conjugate, it may provide useful information concerning the locus of drug or disease state interactions in the presence of significant ER.

The relatively weak relationship between V_R and F_R, as compared to that between V_R and MRT_R, was somewhat unexpected. However, several parameters in the ER model (gut transit rate constants and the rate constant for reabsorption) influence both V_R (through AUC_T and $AUMC_T$) and MRT_R (through the rate of ER loop transit). While these parameters affect the rate of recirculation, they do not influence the cumulative fraction recirculated. Thus, factors that influence ER transit (gastrointestinal motility, hydrolysis of the glucuronide conjugate, reabsorption of liberated parent) would be expected to affect V_R and MRT_R in parallel without altering F_R.

As a demonstration of the utility of the analytical approaches described above in the absence of a distinct ER peak, published concentration-time data for diflunisal (2) and methylergometrine (20) were analyzed to estimate the probable degree of ER. These estimates were then compared to the experimentally derived values reported in these communications. The concentration-time data subjected to analysis are displayed in Fig. 17. For diflunisal, the *AUC* analysis proposed in the present communication indicated that 24.6% of the administered dose would undergo at least one ER cycle. The experimentally derived estimate for the fraction of the dose available for one recirculation was 27.4% (2). In the case of methylergometrine, the predicted value of f_r (26%) also corresponded well to the

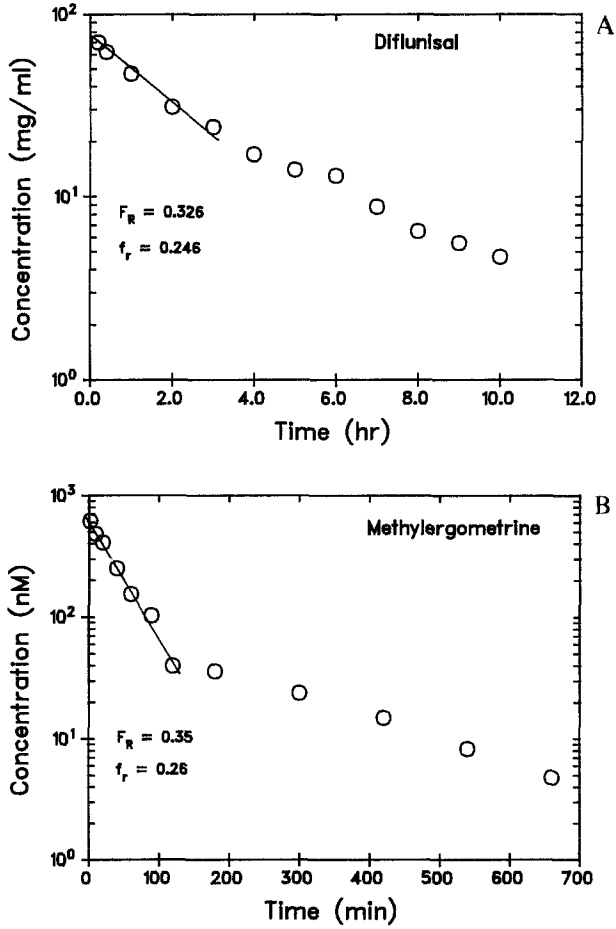

Fig. 17. Concentration-time data for diflunisal and methylergometrine subjected to ER analysis. Solid lines indicate prerecirculatory phase. Data obtained from refs. 2 and 20, respectively.

value calculated by comparing systemic clearance in bile duct-cannulated rats and intact animals (28.6%). In addition to the calculation of traditional kinetic parameters, these data support the use of the analytical approaches described in this report to estimate the contribution of ER to overall systemic disposition.

One aspect of the current recirculatory model that is worthy of particular note is that it predicts that peak serum concentrations of *recirculated* VPA will occur relatively late (approx. 5 hr following administration of the dose). This delay in the appearance of recirculated drug is somewhat surprising

in light of the relatively short initial half-life of VPA (approx. 15 min) and the fact that, in bile duct-cannulated animals, peak biliary concentrations of VPA-G were achieved within 15 min (data not shown). An explanation for the delayed recirculation of VPA is provided by the work of Dickinson *et al.* (32) in which VPA-G was delivered to the intestines of rats via bile duct cannulas. Peak serum concentrations of VPA were attained at 5 to 7 hr following initiation of a 2-hr intrabiliary infusion of the β-glucuronidase-sensitive form (i.e., the relevant metabolite *in vivo*) of the glucuronide conjugate. *In vitro* experiments indicated that VPA-G hydrolysis was approximately seven-fold higher in the cecum, and two- to three-fold higher in the colon, as compared to the small intestine, consistent with the slow input of VPA into serum. Thus, VPA-G appears to be hydrolyzed preferentially in the distal portion of the gastrointestinal tract, probably by β-glucuronidase of bacterial rather than mammalian origin. The ability of the present recirculatory model to predict the time course of VPA in the systemic circulation following delivery of the conjugate directly into the gastrointestinal tract was assessed utilizing the data of Dickinson *et al.* (32). The published data were corrected for the 2-hr infusion time, and the dose administered in the model was changed from previous simulations to deliver 100 mg (VPA equivalents) of the glucuronide conjugate into the recirculatory

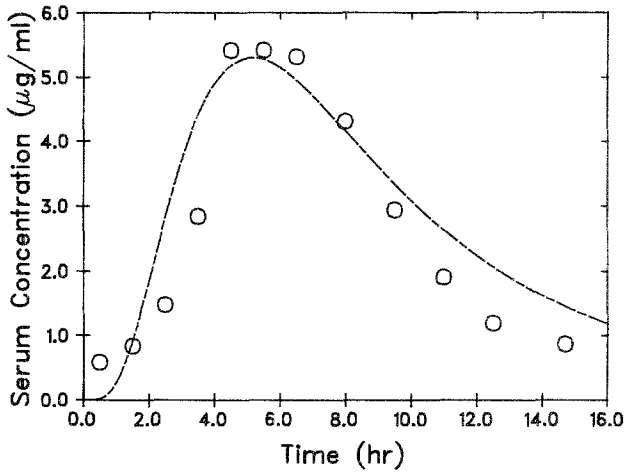

Fig. 18. Comparison of serum VPA concentrations following direct administration of VPA-G into the bile duct (circles) and the predicted concentration–time profile based upon the recirculatory model (line). Data points from Dickinson *et al.* (32) were corrected for a 2-hr infusion. The dose utilized in the model simulation was adjusted to deliver 100 mg (VPA equivalents) of the glucuronide conjugate into the recirculatory loop.

loop. All other parameters of the model were held constant at the values listed in Table I, Simulation 1. Comparison of the model prediction with the data obtained from the literature is provided in Fig. 18. The present recirculatory model accurately predicted both the peak serum VPA concentration and the time to peak. The model overpredicted the initial rate of appearance of liberated parent in the systemic circulation, perhaps due to the assumption of first-order transit of VPA-G through the gastrointestinal tract. Modification of the model to constant-rate gastrointestinal transit may improve the description of the recirculatory data. However, considering the difference in experimental protocols, the description of the data provided by the model was remarkably good.

REFERENCES

1. B. E. Dahlstrom and L. K. Paalzow. Pharmacokinetic interpretation of the enterohepatic recirculation and first-pass elimination of morphine in the rat. *J. Pharmacokin. Biopharm.* **6:**505-519 (1978).
2. J. H. Lin, K. C. Yeh, and D. E. Duggan. Effect of enterohepatic circulation on the pharmacokinetics of diflunisal in rats. *Drug Metab. Dispos.* **13:**321-326 (1985).
3. R. J. Herman, J. D. Van Pham, and C. B. N. Szakacs. Disposition of lorazepam in human beings: Enterohepatic recirculation and first-pass effect. *Clin. Pharmacol. Ther.* **46:**18-25 (1989).
4. F. L. S. Tse, F. Ballard, and J. Skinn. Estimating the fraction reabsorbed for drugs undergoing enterohepatic circulation. *J. Pharmacokin. Biopharm.* **10:**455-461 (1982).
5. R. G. Dickinson, R. C. Harland, A. M. Ilias, R. M. Rodgers, S. N. Kaufman, R. K. Lynn, and N. Gerber. Disposition of valproic acid in the rat: Dose-dependent metabolism, distribution, enterohepatic recirculation, and choleretic effect. *J. Pharmacol. Exp. Ther.* **211:**583-595 (1979).
6. K. Singh, J. M. Orr, and F. S. Abbott. Pharmacokinetics and enterohepatic circulation of 2-*n*-propyl-4-pentenoic acid in the rat. *Drug Metab. Dispos.* **16:**848-852 (1988).
7. O. J. McAnena, M. Rossi, B. M. Mehta, and J. M. Daly. Alteration of methotrexate metabolism in rats by administration of an elemental liquid diet. I. Changes in drug enterohepatic circulation. *Cancer* **59:**31-37 (1987).
8. K. C. Kwan, G. O. Breault, E. R. Umbenhauer, F. G. McMahon, and D. E. Duggan. Kinetics of indomethacin absorption, elimination, and enterohepatic circulation in man. *J. Pharmacokin. Biopharm.* **4:**255-280 (1976).
9. T. R. D. Elmhirst, J. K. Chipman, O. Ribeiro, P. C. Hirom, and P. Millburn. Metabolism and enterohepatic circulation of benzo(*a*)pyrene-4,5-epoxide in the rat. *Xenobiotica* **15:**899-906 (1985).
10. H. Kurebayashi, A. Tanaka, and T. Yamaha. Metabolism and disposition of the flame retardant plasticizer, tri-*p*-cresyl phosphate, in the rat. *Toxicol. Appl. Pharmacol.* **77:**395-404 (1985).
11. D. E. Duggan, K. F. Hooke, R. M. Noll, and K. C. Kwan. Enterohepatic circulation of indomethacin and its role in intestinal irritation. *Biochem. Pharmacol.* **25:**1749-1754 (1975).
12. R. Gugler and G. E. von Unruh. Clinical pharmacokinetics of valproic acid. *Clin. Pharmacokin.* **5:**67-83 (1980).
13. F. Schobben and E. van der Kleijn. Valproate biotransformation. In D. M. Woodbury, J. K. Penry, and C. E. Pippinger (eds.), *Antiepileptic Drugs*, Raven, New York, 1982, pp. 567-578.
14. A. Rescigno and G. Segre. *Drug and Tracer Kinetics*, Blaisdell, Waltham, MA, 1966.

15. J. Barre, J. M. Chamouard, G. Houin, and J. P. Tillement. Equilibrium dialysis, ultrafiltration, and ultracentrifugation compared for determining the plasma-protein-binding characteristics of valproic acid. *Clin. Chem.* **31**:60–64 (1985).
16. W. Loscher. Rapid determination of valproate sodium in serum by gas–liquid chromatography. *Epilepsia* **18**:782–787 (1978).
17. W. Loscher and H. Esenwein. Pharmacokinetics of sodium valproate in dog and mouse. *Arzneim. Forsch.* **28**:782–787 (1978).
18. H. Akaike. An information criterion. *Math. Sci.* **14**:5–9 (1976).
19. M. Gibaldi and D. Perrier. *Pharmacokinetics*, 2nd ed. Marcel Dekker, New York, 1985.
20. U. Bredberg and L. Paalzow. Pharmacokinetics of methylergometrine in the rat: Evidence for enterohepatic recirculation by a linked-rat model. *Pharm. Res.* **7**:14–20 (1990).
21. G. M. Pollack. Pharmacokinetic factors contributing to the nonlinear disposition of valproic acid in the rat. *Pharm. Res.* **3**:145 (1986).
22. G. D. Anderson, A. Acheampong, A. J. Wilensky, and R. H. Levy. Effect of valproate (VPA) dose on formation of hepatotoxic metabolites. *Clin. Pharmacol. Ther.* **47**:130 (1990).
23. P. veng Pedersen and R. Miller. Pharmacokinetics of doxycycline reabsorption. *J. Pharm. Sci.* **69**:204–207 (1980).
24. J.-L. Steimer, Y. Plusquellec, A. Guillaume, and J.-F. Boisvieux. A time-lag model for pharmacokinetics of drugs subject to enterohepatic circulation. *J. Pharm. Sci.* **71**:297–302 (1982).
25. Y. Plusquellec and L. Bousquet. Time-delay for two-compartment models used for study of enterohepatic circulation of drugs. *IEEE Trans. Biomed. Eng.* **6**:469–472 (1984).
26. T. A. Shepard, D. J. Gannaway, and G. F. Lockwood. Accumulation and time to steady state for drugs subject to enterohepatic cycling: A simulation study. *J. Pharm. Sci.* **74**:1331–1333 (1985).
27. W. A. Colburn. Pharmacokinetic analysis of concentration-time data obtained following administration of drugs that are recycled in the bile. *J. Pharm. Sci.* **73**:313–317 (1984).
28. J. G. Wagner, A. R. DiSanto, W. R. Gillespie, and K. S. Albert. Reversible metabolism and pharmacokinetics: Application to prednisone–prednisolone. *Res. Comm. Chem. Path. Pharmacol.* **32**:387–405 (1981).
29. S. Hwang, K. C. Kwan, and K. S. Albert. A linear model of reversible metabolsim and its application to bioavailability assessment. *J. Pharmacokin. Biopharm.* **9**:693–709 (1981).
30. W. F. Ebling and W. J. Jusko. The determination of essential clearance, volume, and residence time parameters of recirculating metabolic systems: The reversible metabolism of methylprednisolone and methylprednisone in rabbits. *J. Pharmacokin. Biopharm.* **14**:557–599 (1986).
31. H. Cheng and W. J. Jusko. Mean residence times of multicompartmental drugs undergoing reversible metabolism. *Pharm. Res.* **7**:103–107 (1990).
32. R. G. Dickinson, R. M. Kluck, M. J. Eadie, and W. D. Hooper. Disposition of β-glucuronidase-resistant "glucuronides" of valproic acid after intrabiliary administration in the rat: Intact absorption, fecal excretion, and intestinal hydrolysis. *J. Pharmacol. Exp. Ther.* **233**:214–221 (1985).